

Supporting Information

Interplay of the adsorption of light and heavy paraffins in hydroisomerization over H-Beta zeolite

Pedro S. F. Mendes^{a,b,1*}, Céline Chizallet^b, Javier Pérez-Pellitero^b, Pascal Raybaud^b, João M. Silva^{a,c}, M. Filipa Ribeiro^a, Antoine Daudin^b, Christophe Bouchy^{b*}

^a*Centro de Química Estrutural, Instituto Superior Técnico, Universidade de Lisboa, Av. Rovisco Pais, 1049-001 Lisboa, Portugal*

^b*IFP Energies nouvelles, Rond-point de l'échangeur de Solaize, BP 3, 69360 Solaize, France*

^c*ADEQ-ISEL, Instituto Superior de Engenharia de Lisboa, Instituto Politécnico de Lisboa, R. Cons. Emídio Navarro, 1959-007 Lisboa, Portugal*

* pedro.f.mendes@tecnico.ulisboa.pt; christophe.bouchy@ifpen.fr ; +33 (0)4 37 70 28 60.

S1 – GCMC simulations.....	2
S2 – Hydroconversion of <i>n</i> -hexadecane.....	7
S3 – Macrokinetic model.....	9
References.....	12

¹ Present address: Laboratory for Chemical Technology, Ghent University, B-9052 Ghent, Belgium.

S1 - GCMC simulations

General information

GCMC (Grand Canonical Monte Carlo) simulations combined with a bias scheme for the insertion of the centre of mass of the guest molecules were performed to calculate the adsorption isotherms with the GIBBS code v.9.3. Production runs consist of at least 10 million MC steps for pure compounds, and 50 million steps for mixtures. The atomic positions of the solid were frozen during the simulations. This allowed the construction of a guest-host interaction energy grid prior to the MC simulations. All simulations were performed in a simulation box incorporating 9 unit cells for BEA (3×3×3 purely siliceous cell, A polymorph). LJ interactions were calculated using a cutoff radius of 37.98 Å. No Lennard-Jones tail corrections were considered. The crystallographic positions of the different atoms were taken from the IZA database (<http://www.iza-structure.org/databases/>).

Adsorption data for *n*-hexadecane

The physisorption Langmuir isotherm for *n*-hexadecane in H-Beta zeolite at 538 K was calculated based on the experimental data and semi-empirical model proposed by Denayer et al [1]. The adsorption equilibrium constant at 538 K (working temperature of Denayer's study) was estimated for *n*-hexadecane (carbon number CN=16) through Eq. S1. The enthalpy of adsorption was estimated through Eq. S2.

$$K = A \cdot e^{(B)(CN)} \quad \text{Equation S1}$$

$$-\Delta H_0 = \alpha \cdot CN + \beta \quad \text{Equation S2}$$

Table S1: Parameters for adsorption model obtained from [1].

Parameter	Value	Units
A	7.44×10^{-8}	mol kg ⁻¹ Pa ⁻¹
B	1.07	-
α	10.0	kJ mol ⁻¹
β	2.58	kJ mol ⁻¹

The adsorption equilibrium constant was then estimated at 538 K through Van't Hoff equation (Eq. S3). The value obtained was 77.6 Pa⁻¹.

$$K_1 = K_2 \cdot e^{\frac{-\Delta H_0}{R} \left(\frac{1}{T_1} - \frac{1}{T_2} \right)} \quad \text{Equation S3}$$

In Fig. S1, the adsorption isotherm at 538 K corresponding to the estimated parameters is plotted. For comparison purposes, the adsorption isotherm of *n*-octane in zeolite Beta is also shown, according to the available data [1].

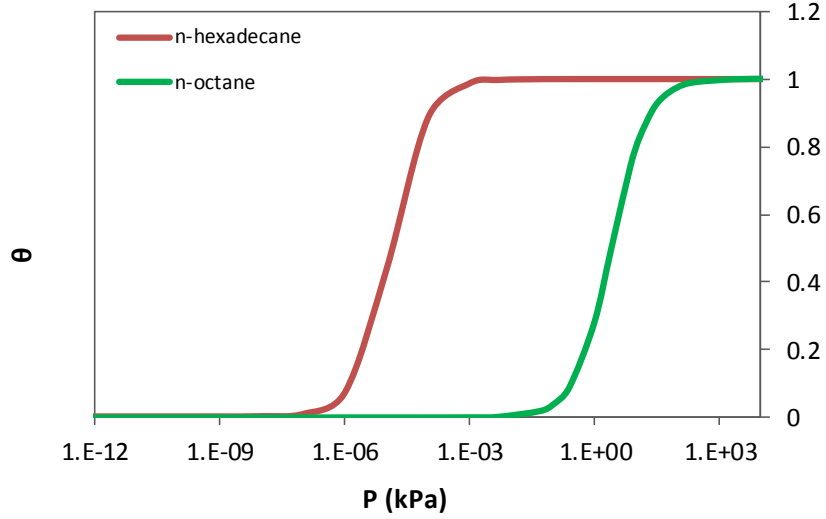


Figure S1: Langmuir adsorption isotherms for *n*-C₈H₁₈ and *n*-C₁₆H₃₄ in zeolite Beta at 538 K estimated according to Eq. S3. Parameters for *n*-C₈H₁₈ obtained in [1] based on experimental data. Parameters for *n*-C₁₆H₃₄ extrapolated from [1] based on Eqs. S1 and S2.

Models used in GCMC simulations:

Since the zeolite *BEA zeolite is assimilated to be purely siliceous, the energetic description of the system is only based on the summation of two different contributions :

$$U_{TOT} = U_{LJ} + U_{intra} \quad \text{Equation S4}$$

where the term corresponding to the dispersion-repulsion energy is described *via* a Lennard-Jones potential :

$$U_{LJ}^{ij}(r) = 4 \varepsilon \left[\left(\frac{\sigma_{ij}}{r_{ij}} \right)^{12} - \left(\frac{\sigma_{ij}}{r_{ij}} \right)^6 \right] \quad \text{Equation S5}$$

A collection of intramolecular terms allow to account for the energetic contribution associated to the internal deformation/flexibility of the hydrocarbons :

$$U_{intra} = U_{bonding} + U_{bending} + U_{torsion} =$$

$$= \sum_{i=1}^{n_{bonds}} \frac{1}{2} k_b^i (d - d_0)^2 + \sum_{i=1}^{n_{angles}} \frac{1}{2} k_a^i (\cos \theta - \cos \theta_0)^2 + \sum_{i=1}^{n_{dihedral\ angles}} \sum_{j=1}^8 A_i^j (\cos \chi)^j$$

Equation S6

The different parameters used in the calculations are compiled in the following tables :

Table S2: Lennard-Jones parameters

Force center	σ^\dagger [Å]	ϵ^\dagger [K]	$\delta^{\dagger\dagger}$ [Å]
CH₃-AUA	3.6072	120.15	0.21584
CH₂-aliph-AUA	3.4612	86.291	0.38405
CH-aliph-AUA	3.3625	50.98	0.64599
C-aliph-AUA	2.440	15.035	0.00000
O-zeolite	3.00	112.236	----
Si-zeolite	0.00	0.00	----

[†]Lorentz-Berthelot mixing rules were employed to determine the interactions between different force center types.

^{††} δ is the anisotropic distance used in the AUA (Anisotropic United Atoms) potential. □

Table S3: Parameters of the harmonic bonding potential

Bond	k_b [K]	d_0 [Å]
CH ₃ -AUA ---- CH ₂ -aliph-AUA	0.0	1.535
CH ₃ -aliph-AUA ---- CH-aliph-AUA	0.0	1.535
CH ₂ -aliph-AUA ---- CH ₂ -aliph-AUA	0.0	1.535
CH ₂ -aliph-AUA ---- CH-aliph-AUA	0.0	1.535
CH ₂ -aliph-AUA ---- C-aliph-AUA	0.0	1.540
CH ₃ -AUA ---- C-aliph-AUA	0.0	1.540

Table S4: Parameters of the harmonic bending potential

Angle	k_a [K]	θ_0 [deg]
CH3-AUA ---- CH2-aliph-AUA ---- CH2-aliph-AUA	74900	114.00
CH2-aliph-AUA ---- CH2-aliph-AUA ---- CH2-aliph-AUA	74900	114.00
CH2-aliph-AUA ---- CH2-aliph-AUA ---- CH-aliph-AUA	74900	114.00
CH3-AUA ---- CH-aliph-AUA ---- CH2-aliph-AUA	72700	112.00
CH2-aliph-AUA ---- CH-aliph-AUA ---- CH2-aliph-AUA	72700	112.00
CH2-aliph-AUA ---- CH2-aliph-AUA ---- C-aliph-AUA	74900	114.00
CH3-AUA ---- C-aliph-AUA ---- CH2-aliph-AUA	70311	109.47
CH3-AUA ---- C-aliph-AUA ---- CH2-aliph-AUA	70311	109.47
CH3-AUA ---- C-aliph-AUA ---- CH3-AUA	70311	109.47
C-aliph-AUA ---- CH2-aliph-AUA ---- CH-aliph-AUA	74900	114.00

Table S5: Parameters of the torsion potential

Dihedral angle	Angle	A^0	A^1	A^2	A^3	A^4	A^5	A^6	A^7	A^8
(*) – CH2-aliph-AUA – CH2-aliph-AUA -- (*)	0	1001.36	2129.52	-303.06	-3612.27	2226.71	1965.93	-4489.34	-1736.22	2817.37
(*) – CH-aliph-AUA – CH2-aliph-AUA -- (*)	0	373.05	919.04	268.15	-1737.21	0	0	0	0	0
(*) – C-aliph-AUA – CH2-aliph-AUA -- (*)	0	230.65	691.92	0	-922.58	0	0	0	0	0

Results for 1:1:2:4 mixture

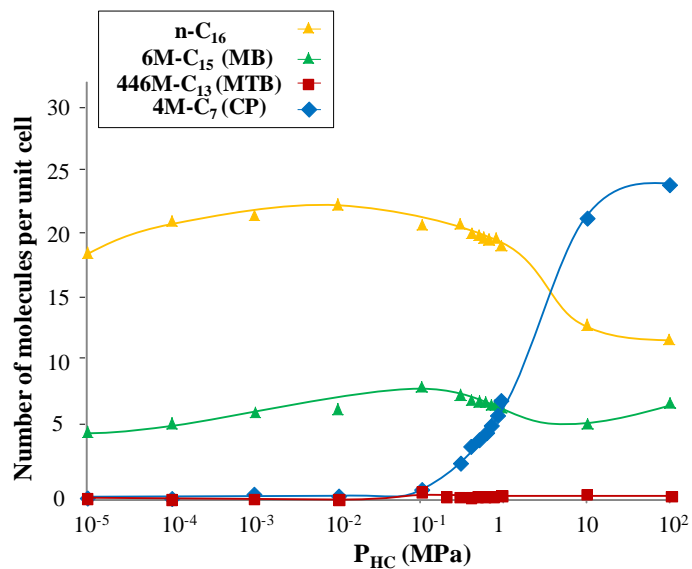


Figure S2: Adsorption isotherms at 538 K obtained from GCMC calculations, for n-C₁₆:6M-C₁₅:446M-C₁₃:4M-C₇ mixtures, representative of n-C₁₆:MB:MTB:CP ones. Concentration ratio in gas phase: 1:1:2:4. Lines are only guides for the eye. The “low” and “high” pressures conditions corresponds to about 10⁻¹ and 4.10⁻¹ MPa respectively in this model.

S2 - Hydroconversion of *n*-hexadecane

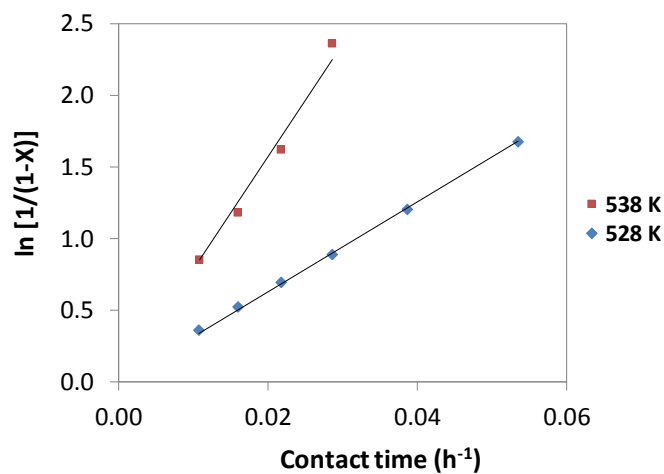


Figure S3: Yield of feed isomers as function of *n*-hexadecane conversion for Pt/H-Beta catalyst at 4.1 MPa of total pressure.

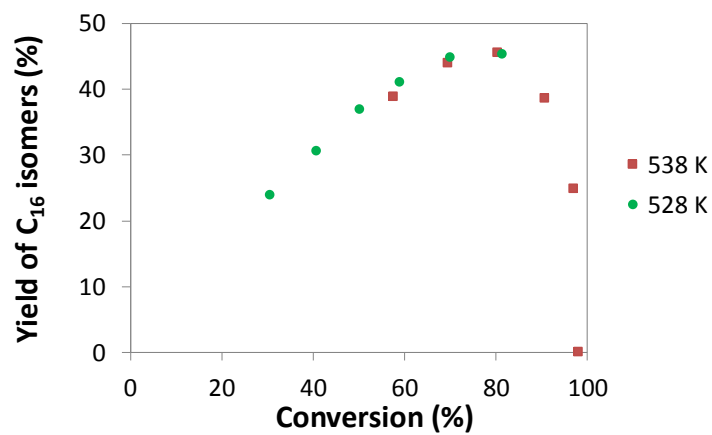


Figure S4: Yield of feed isomers as function of *n*-hexadecane conversion for Pt/H-Beta catalyst at 4.1 MPa of total pressure.

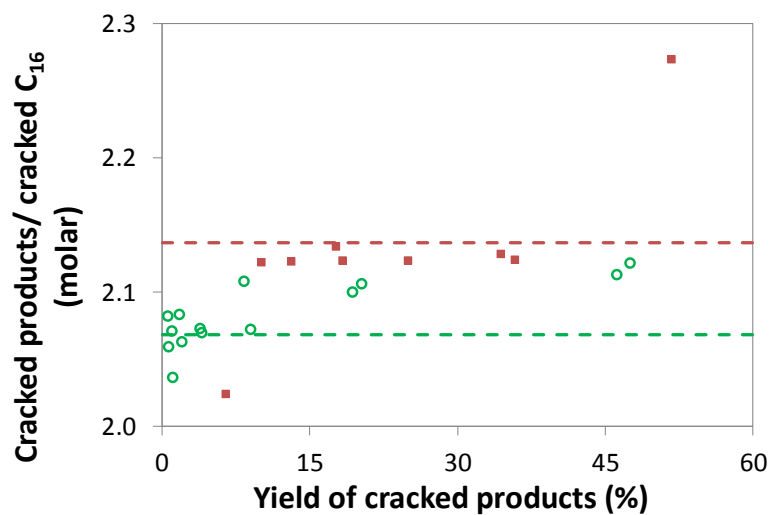


Figure S5: Overcracking index as function of the cracked products yield at at 1.1 (○) and 4.1 MPa (■) of total pressure. Dashed lines correspond to the average value.

S3 - Macrokinetic model

Concentration profile as function of conversion

For two consecutive unimolecular reactions (Scheme S1), the concentration profiles in a plug-flow with invariant number of moles and pure feeding of A is given by Equations S7 and S8 according to Levenspiel's textbook [2]. The profiles are a function of the kinetic constants for both reactions k_1 and k_2 , contact time τ , and initial concentration of A C_{A0} .



$$\frac{C_A}{C_{A0}} = e^{-k_1\tau} \quad \text{Equation S7}$$

$$\frac{C_B}{C_{A0}} = \frac{1}{k_2/k_1 - 1} (e^{-k_1\tau} - e^{-k_2\tau}) \quad \text{Equation S8}$$

Writing Eq. S1 in order to τ and replacing it in Eq. S2, the concentration profile of B becomes function of the concentration of A. By replacing C_A by the definition of conversion, the concentration profile of B be obtained as function of conversion (Eq. S9).

$$\frac{C_B}{C_{A0}} = \frac{1}{k_2/k_1 - 1} \left[(1-x) - (1-x)^{k_2/k_1} \right] \quad \text{Equation S9}$$

Application to the hydroconversion of *n*-hexadecane

The derivation of the abovementioned concentration profiles is subjected to two conditions: invariant number of moles (and, thereby, volume) throughout the reactor and first-order reactions.

Concerning the first condition, the two reactions involved are isomerization (Scheme S2) and cracking (Scheme S3). Both reactions do not affect the total number of moles.



Obviously, the reactions shown are global reactions, and not elementary steps, thus the molecularity of the mechanism cannot be derived from those. According to the classical bifunctional mechanism for hydroconversion of alkanes [3], for

a well-balanced catalyst (i.e. hydrogenation/de-hydrogenation reactions in equilibria), the apparent reaction rate is first-order in the reacting alkane [4,5]. This has been also verified experimentally [5-7]. Therefore, for *n*-hexadecane, the apparent reaction scheme can be represented by Scheme 4 and the corresponding concentration profile for the C₁₆ isomers, which corresponds as well to the yield, by Eq. S4.



$$Y_{i-C_{16}} = \frac{F_{i-C_{16}}}{F_{C_{n-C_{16}}}^0} = \frac{1}{k_{\text{crack}}/k_{\text{isom}} - 1} \left[(1-x) - (1-x)^{k_{\text{crack}}/k_{\text{isom}}} \right] \quad \text{Equation S10}$$

It is also worth mentioning that the reaction order on the hydrogen is typically -1. The apparent kinetic constants include, thus, a term on the partial pressure of hydrogen. Under our (typical) hydroconversion conditions, H₂ is stoichiometrically in excess. Hence, its partial pressure can be assumed constant. As a result, the ratio of the two constants becomes H₂ pressure independent.

Estimation of $k_{\text{crack}}/k_{\text{isom}}$

For each pressure, $k_{\text{crack}}/k_{\text{isom}}$ was estimated by minimization of the weighed squared residuals between the experimentally observed yields and the model calculated ones (Eq. S10).

$$SSQ = \sum_{j=1}^{n_{\text{exp}}} \omega_j \left[(Y_{i-C_{16}}^{\text{exp}})_j - (Y_{i-C_{16}}^{\text{mod}})_j \right]^2 \quad \text{Equation S11}$$

In order to adequately simulate the maximum of the curve (which is the key process parameter for hydroconversion), the experimental points in the conversion range 60 - 95 % had triple the weight ω than the other points. The sum of the weighed squared residuals was minimized by GRG Nonlinear method available in Microsoft Excel 2013. The corresponding parity diagram is shown in Fig. S6.

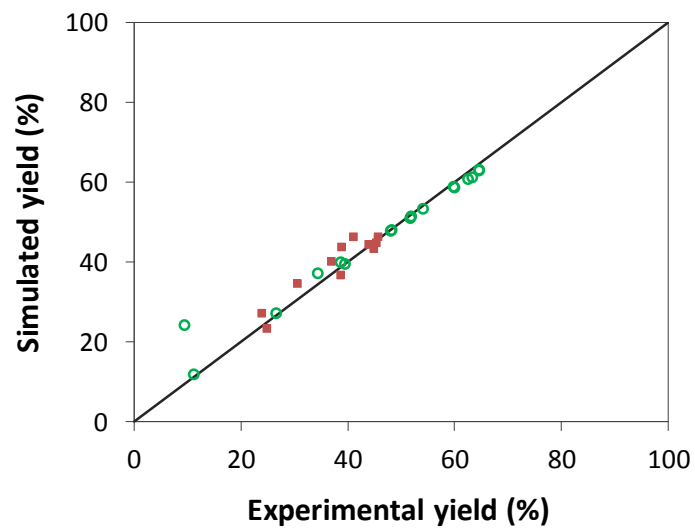


Figure S6: Simulated vs. measured yield of C₁₆ isomers at at 1.1 (○) and 4.1 MPa (■) of total pressure.

References

- [1] J. F. Denayer, G. V. Baron, J. A. Martens, P. A. Jacobs. *J. Phys. Chem. B* 102 (1998) 3077–3081.
- [2] Levenspiel, O. *Chemical Chemical Reaction Engineering*, 3rd Edition; John Wiley & Sons, Ltd: New York, 1999.
- [3] H.L. Coonradt, W.E. Garwood, *Ind Eng Chem Proc Dd* 3 (1964) 38-45.
- [4] P.S.F. Mendes, J.M. Silva, M.F. Ribeiro, P. Duchêne, A. Daudin, C. Bouchy, *AIChE J.* 63 (2017) 2864–2875.
- [5] T.F. Degnan, C.R. Kennedy, *AIChE J.* 39 (1993) 607–614.
- [6] M.J. Girgis, Y.P. Tsao, *Ind. Eng. Chem. Res.* 35 (1996) 386–396.
- [7] V. Calemma, S. Peratello, C. Perego, *Appl. Catal. A* 190 (2000) 207–218.